JOURNAL OF CHEMICAL INFORMATION AND MODELING

ARTICLE

pubs.acs.org/jcim

Detailed Mechanism of Squalene Epoxidase Inhibition by Terbinafine

Marcin Nowosielski,[*,†] Marcin Hoffmann,[*,‡] Lucjan S. Wyrwicz,[†,§] Piotr Stepniak,[†] Dariusz M. Plewczynski,[⊥] Michal Lazniewski,[⊥,∥] Krzysztof Ginalski,[⊥] and Leszek Rychlewski[†]

[†]BioInfoBank Institute, Limanowskiego 24A, 60-744 Poznań, Poland

[‡]Quantum Chemistry Group, Department of Chemistry, Adam Mickiewicz University, Grunwaldzka 6, 60-780 Poznań, Poland

[§]Laboratory of Bioinformatics and Systems Biology, M. Sklodowska-Curie Cancer Center and Institute of Oncology, WK Roentgena 5, 02-781 Warsaw, Poland

[⊥]Laboratory of Bioinformatics and Systems Biology, Interdisciplinary Centre for Mathematical and Computational Modelling, University of Warsaw, Pawinskiego 5a, 02-106 Warsaw, Poland

[∥]Department of Physical Chemistry, Faculty of Pharmacy, Medical University of Warsaw, Banacha 1, 02-097 Warsaw, Poland

Supporting Information

ABSTRACT: Squalene epoxidase (SE) is a key flavin adenine dinucleotide (FAD)-dependent enzyme of ergosterol and cholesterol biosynthetic pathways and an attractive potential target for drugs used to inhibit the growth of pathogenic fungi or to lower cholesterol level. Although many studies on allylamine drugs activity have been published during the last 30 years, up until now no detailed mechanism of the squalene epoxidase inhibition has been presented. Our study brings such a model at atomic resolution in the case of yeast *Saccharomyces cerevisiae*. Presented data resulting from modeling studies are in excellent agreement with experimental findings. A fully atomic three-dimensional (3D) model of squalene epoxidase (EC 1.14.99.7) from *S. cerevisiae* was built with the help of 3D-Jury approach and further screened based on data known from mutation experiments leading to terbinafine resistance. Docking studies followed by molecular dynamics simulations and quantum interaction energy calculations [MP2/6-31G(d)] resulted in the identification of the terbinafine−squalene epoxidase mode of interaction. In the energetically most likely orientation of terbinafine its interaction energy with the protein is ca. 120 kJ/mol. In the favorable position the terbinafine lipophilic moiety is located vertically inside the squalene epoxidase binding pocket with the *tert*-butyl group oriented toward its center. Such a position results in the SE conformational changes and prevents the natural substrate from being able to bind to the enzyme's active site. That would explain the noncompetitive manner of SE inhibition. We found that the strongest interaction between terbinafine and SE stems from hydrogen bonding between hydrogen-bond donors, hydroxyl group of Tyr90 and amine nitrogen atom of terbinafine. Moreover, strong attractive interactions were recorded for amino acids whose mutations resulted in terbinafine resistance. Our results, elucidating at a molecular level the mode of terbinafine inhibitory activity, can be utilized in designing more potent or selective antifungal drugs or even medicines lowering cholesterol in humans.

INTRODUCTION

Squalene epoxidase (SE; EC 1.14.99.7) is a key flavin adenine dinucleotide (FAD)-dependent enzyme of ergosterol and cholesterol biosynthetic pathways that catalyzes the stereospecific epoxidation of squalene to 2,3-(*S*)-oxidosqualene, including fungi[1] and mammalia.[2] It is therefore an attractive potential target for drugs used to inhibit the growth of pathogenic fungi or to lower the cholesterol level. As cholesterol-lowering drugs are among the top earners among known pharmaceuticals, the mamalian SE has been the subject of extensive investigations since 1970.[2−4] Although fungi SE enzyme preparations from *Saccharomyces cerevisiae*[1] and pathogenic yeast *Candida albicans*[5] were described over 10 years later, the first study on a new allyamine drug acting as the squalane epoxidase inhibitor was published already in 1981.[6] Naftifine[6] and terbinafine (SF 86-327 compound)[7] were found to block ergosterol biosynthesis inter alia in *S. cerevisiae* and dermatophytes, such as *C. ablicans*, by inhibiting the SE in a noncompetitive manner.[8] Currently terbinafine and nafitifine are considered topical (terbinafine also systemic) antifungal drugs and are sold under different brand names.

One should notice that although many varied studies on the terbinafine and naftifine activity have been published during the last 30 years, the inhibition mechanism model has not been presented. There are no crystal structures for SEs available, and the domains responsible for enzymatic activity as well as inhibitor−enzyme interactions are not well understood. Although a theoretical three-dimensional (3D) model for the *S. cerevisie* SE has been shown, it is not easily available.[9] The only enzyme in this class of flavoproteins for which the 3D structure is known is *p*-hydroxybenzoate hydroxylase (PHBH, PDB code 1PBE) of *Pseudomonas fluorescens*.[10] PHBH contains two FAD fingerprint motifs (FADI and FADII) and a conserved sequence motif with a putative dual function in the FAD/NAD(P)H binding.[11] These domains are also found in SEs.

Received: October 15, 2010
Published: January 13, 2011

Studies on the human SE enzyme (gene located on chromosome 8q24.1)[12] until the mid-1990s remained limited to those carried out with subcellular preparations from HepG2 cells.[13,14] The first mammalian SE sequence (rat) was reported in 1995, which was followed by the cloning of mouse and human SE.[15,16] Rat SE exhibited limited sequence similarity to the yeast enzymes (30%) and to the other flavoproteins, while the sequence homology between the rat and the human squalene monooxygenase amounts to 84% . Likewise in the case of fungi, structural details of these enzymes from X-ray diffraction studies are not available. Many efforts and great resources have been involved in the research on human SE inhibitors, especially because blocking cholesterol synthesis at this step may result in the accumulation of squalene only, which is known to be stable and nontoxic. The synthesis of several potent, most likely orally bioavailable inhibitors of SE, has been reported by Banyu Pharmaceutical, Yamonuchi, Pierre Fabre, and Fujisawa.[17−22] However it has been 20 years since the first study was published, and so far there is an absolute lack of information about results from clinical trials. Moreover 40 years since the first report on mammalian SE was published, neither inhibition mechanism nor structural data are known.

Because in neither case (fungi nor mammalian) detailed mechanism of SE inhibition is known, our aim was to proposed such a mechanism. We decided to perform simulations for the best experimentally described case—inhibition of SE by terbinafine with yeast *S. cerevisiae*—and obtained results corresponding well with the experimental data. Due to the high sequence similarity between yeast enzymes and their ca. 30% sequence similarity to the mammalian SE, provided information has a wider usage, also for other organisms. Consequently the study may be found to be not only intellectually absorbing but also very useful.

COMPUTATIONAL PROCEDURE

S. cerevisiae SE model was built based on 2QA1[23] and 1PBE[24] templates, and the 3D-Jury[25] approach was used for the initial fold assignment. 3D-Jury takes as input groups of models generated by a set of fold assignment servers, neglecting the confidence scores assigned by the servers to the models, and uses its own unique scoring functions. The application of the 3D-Jury approach on the sequence of typical for this class of FAD-dependent enzymes with two domain structure[10] resulted in the selection of models. In order to obtain the full atom 3D structure, the side-chains and the missing loops were rebuilt with the Modeler program.[26] Side chains were optimized using the CHARMM 22 force field.[27]

In the next step, a docking procedure was carried out with the AutoDock 4 software.[28] First we used the MolConvert plugin[29] to generate different terbinafine conformers and chose the lowest-energy structure. Additionally a second conformer was selected to have the highest root-mean-square deviation (rmsd) from the first one. These two structures differed in the absolute configuration of the nitrogen atom and were used as the entry for the AutoDock, which further generated their different conformers during the genetic algorithm runs. Docking was performed with a grid box narrowing the accepted space to that experimentally pointed as important in interactions with the ligand.[30] Dockings have been run in eight sets for each of the two different terbinafine enantiomers, with parameter changes to examine any differences they might provide. Docking sets 1−4 had a grid box restricted to the probable inhibitor binding pocket and 5−8 had the grid box enlarged to include active sites positioned deeper in the protein. Additionally in docking sets 2, 3, 7, and 8, van der Waals radii of terbinafine atoms were doubled. In all, we obtained 320 different terbinafine poses (160 for each enantiomer, 20 from each parameter set).

Because results obtained in the seventh and eighth docking series were in clear contradiction with the available experimental data, they were neglected with the exception of one terbinafine position, significantly different from the other docking series. Among the remaining docked positions the best one (according to the AutoDock score) for each of the six different parameter sets was chosen (overall six positions). Selected positions were superimposed, and four of them were found unique (rmsd > 0.2 Å). Each of the five different terbinafine molecule positions in the SE binding pocket was considered as a different inhibitor−enzyme system, and the following computational procedures were carried out separately for each system.

Molecular dynamic simulations were done through the parallel program NAMD 2.7b1,[31] and MD data were analyzed using VMD software.[32] For the SE protein, the CHARMM 22[27] force field was used, and for terbinafine, CGenFF[33] (the CHARMM compatible force field for a drug-like molecules) was used. The cutoff of 12 Å for the van der Waals interactions and the real space electrostatic interactions was set up. The switching distance equaled 10 Å, and the pair list distance equaled 13.5 Å. The default value of 1 fs time step was used, each cycle containing 10 steps. No water molecules or ions were added to the system to keep the consistency with the next study phase, a quantum mechanical calculation in vacuum. The initial structures were minimized without any constrains for the SE atoms. There were also no constrains for the terbinafine atoms. Minimizations were carried out until the convergence criteria were reached—change of all atoms rmsd < 0.01 Å during 1000 steps. The molecular dynamic simulation was performed for the initial temperature of 273.15 K for the system, and during the last 1000 steps, all atom coordinates were written, then the mean values were calculated.

Next single point quantum mechanics energy calculations for chosen amino acid−terbinafine pairs were carried out. Quantum mechanics (QM) region size was defined by the distance from the terbinafine molecule, and these amino acids were included for which at least one atom was in the range of 5 Å from any of the terbinafine atoms, in any of the different terbinafine positions. The distance of 5 Å was chosen as the limit of known efficient nonbonded inhibitor−enzyme interactions.[34] In all we calculated interaction energies for 48 terbinafine−amino acid pairs for each different terbinafine orientation in the SE binding pocket. The single point energy calculations were performed using the Gaussian03 program,[35] and the MP2 method[36] combined with the 6-31G(d) basis set[37] was used. The interaction energies were computed with the usual counterpoise correction.[38] To estimate the influence of the hydrophobic effect[39] on the protein−ligand complex formation for a chosen terbinafine, position hydrophobic contact surface area has been calculated using the CCP4 software with the default parameter values.[40]

Figures were prepared using UCSF Chimera.[41]

RESULTS AND DISCUSSION

The *S. cerevisiae* SE model exhibits the two-domain structure (the FAD cofactor and the substrate binding) typical for this class of enzymes (Figure 1).[10]

In the FAD cofactor binding domain two FAD fingerprint motifs characteristic for a flavoproteins hydroxylases are present (Figure 2).[11] The first FAD fingerprint, known as the Rossmann

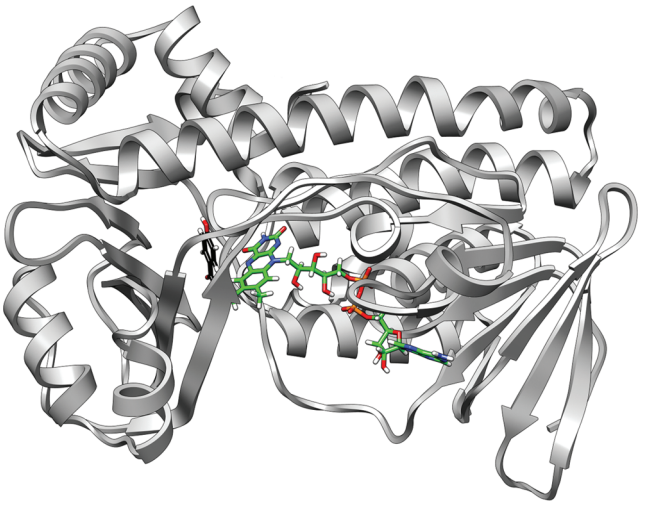

Figure 1. *S. cerevisiae* SE model built based on 2QA1[23] and 1PBE[24] templates. FAD (green) and PHB (p-hydroxybenzoic acid, black) molecules were superimposed from the 1PBE template in order to point out regions of the protein typically responsible for substrate and cofactor binding.

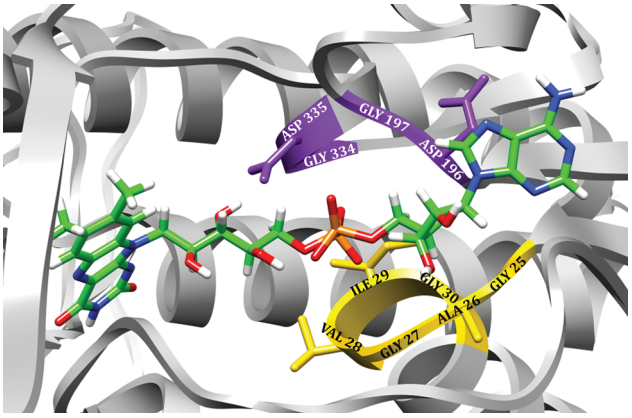

Figure 2. *S. cerevisiae* SE FAD cofactor binding domain. Amino acids comprising the Rossmann fold were marked with gold color. Amino acids belonging to the FAD II fingerprint motif were marked with purple color.

fold, contains the $_{25}$GlyXGlyXXGly$_{30}$ sequence. This is a common motif among the FAD and NAD(P)H-dependent oxidoreductases and usually plays an important role in the binding of a FAD moiety.

In the case of *S. cerevisiae* SE, it was shown that mutations of an amino acids belonging to the FAD I fingerprint motif (Gly27Ser and Gly30Ser) reduce the enzyme in vitro activity. In our model Gly30, Gly25, and Ggly27 are located close to the biphosphate and adenosyl portion of the cofactor. Amino acid highly conserved sequence 209AspGly210 along with Gly334 and Asp335 comprises the second FAD fingerprint motif. These amino acids are also close to the biphosphate and ribitol moieties of the flavin cofactor, however they are located on the opposite side with respect to the Gly25, Gly27, and Gly30.

Based on the model of *S. cerevisiae* SE, further docking studies were conducted to explain the mode of binding of terbinafine to SE. Consequently, two different terbinafine conformers A and B were used, and the docking procedure was carried out for eight different parameter sets. For each terbinafine conformer and each parameter set, 10 `best' (according to AutoDock score) positions into the SE binding pocket were selected. In all we obtained 320 different positions, which could be divided into three main groups. The first group consisted of terbinafine molecules located vertically inside the upper part of SE binding pocket with ene-yne moiety oriented to the protein center. Second group also consisted of terbinafine molecules located vertically inside the upper part of the SE binding pocket, but in this case, the naftalene ring was oriented toward the protein center. Molecules located horizontally inside the lower region of the SE binding pocket comprise the third group. For the larger grid boxes most of highly scored terbinafine docked poses were found in the lower part of an enzyme binding pocket, where the reaction center probably lies. Although there is an entrance leading to the reaction center from the upper part of a binding pocket, it does not seem to be wide enough for the tested inhibitor to come in; it may be wide enough only for squalene. Moreover, experimental studies on SE mutations causing the terbinafine resistance only point to amino acids located in the upper part of enzyme binding pocket as important for the inhibitor binding process.[30] Therefore such results, obtained in seventh and eighth docking series, were neglected. From the rest group of results (obtained from 1−6 parameter sets), one, the best docked terbinafine molecule, position was taken (overall six positions). In all cases the scoring function indicated that the highest binding affinity to the SE enzyme has the B terbinafine conformer. To clearly identify the chosen docking results they were named: T1_B1, T1_B2, ..., T1_B6, according to their best scoring (T1), terbinafine conformation (B), and parameter set (1−6) for which docking procedure was carried out. Selected positions were superimposed, and four of them were found unique (rmsd not greater than 0.2 Å). Docked terbinafine positions T1_B2 and T1_B4 had exactly the same orientation in a SE binding pocket as T1_B1. Because the AutoDock scoring function relies on charged chemical groups and hydrophilic interactions, whereas the ligand tested in this study is in great part hydrophobic, docking results with a lower score were also thoroughly inspected. While the terbinafine position T8_B5 was significantly different from those picked earlier, it was also taken into account. Following, molecular mechanics minimizations for five enzyme−terbinafine systems were carried out. Simulations were done without any constrains for the terbinafine as well as the enzyme atoms. The fastest convergence criteria were meet for the T1_B3 system, after less than 7000 steps. The highest number of steps needed to reach convergence was 40 000 in the case of the T1_B7 system. The rmsd between the starting and the minimized structure varied from 1.7 Å for the T1_B3 to 2.7 Å for the T8_B5 (Table 1).

Subsequently, MD simulations for the previously minimized systems were performed over nanoseconds, and mean values of atomic coordinates through the last 1000 steps were calculated, as suggested by the study of Khandewal.[42] To avoid computational artifacts during the MD simulation, such parameters as rmsd, between the initial and final protein structure, α helices shape as well the number of steps required to meet convergence criteria were thoroughly inspected. Because in docking procedure, starting points of the ligand inside the given grid box are usually random, it is therefore highly probable that a chosen pose would never be observed in vivo. One cannot avoid such distortion. However one may try to avoid a situation in which a protein model is forced to adopt conformation suitable for an

Table 1. Results of Combined MM/QM Calculations for Different Terbinafine Positions Inside the *S. cerevisiae* SE Binding Pocket[a]

position	*E* (kJ/mol)	rmsd (Å)	*N*
T1_B1	−100	2.0	9 500
T1_B3	−117	1.7	7 000
T1_B5	−85	2.2	17 000
T8_B5	482	2.7	40 000
T1_B6	−75	2.4	22 500

[a] E is the calculated interaction energy (MP2/6-31G(d)) between terbinafine and amino acids in the range of 5 Å (see Computational Procedure Section); rmsd is the rmsd between SE structures before and after the MM minimization; and *N* is the number of steps required to meet convergence criteria during the MM minimization.

inappropriate inhibitor position during MD simulation. We believe that MD simulation details, such as rmsd between initial and final protein−ligand system structure and number of steps required to meet convergence criteria, when analyzed by comparison, might be of some help in this case (e.g., a very high number of steps required to meet convergence criteria might stem from inhibitor−enzyme complex instability).

For further, more accurate quantum mechanical calculations, the inhibitor−enzyme complexes had to be divided into smaller parts. In all we calculated interaction energies for 48 terbinafine−amino acid pairs for each different terbinafine orientation in the SE binding pocket. QM region size was defined by the distance from the terbinafine molecule, and these amino acids were included for which at least one atom was in the range of 5 Å from any of the terbinafine atoms, in any of the different terbinafine positions. The distance of 5 Å was chosen as the limit of known efficient nonbonded inhibitor−enzyme interactions.[34] Indeed we observed that calculated interaction energies between terbinafine and amino acids located further than 5 Å from the molecule were weak, up to 1.5 kcal/mol, and usually do not exceed 0.5 kcal/mol. Consequently, increasing the QM region size practically does not affect the results. Decreasing the QM region radii from 5 to 3 Å affects the results, however, the same conclusions can still be drawn. A smaller QM region than this, defined by the radii of 3 Å, does not seem to be justified at all.

Results of the single point energy calculations with the counterpoise correction are presented in Table 1. The data obtained indicate that the SE enzyme binds terbinafine molecule the strongest in the case of T1_B3 system (−117 kJ/mol). On the other hand strong repulsion, clearly indicating inappropriate position inside protein, was observed for T8_B5 system (482 kJ/mol). Attractive inhibitor−enzyme interactions, weaker than for the T3_B1 system at least 17 kJ/mol, were determined for the remaining complexes.

One should notice that calculated interaction energies are not the only factors that make contribution to the overall binding affinity. The protein−ligand complex formation is a complicated thermodynamic process described by many other parameters, such as entropy changes associated with desolvation, decreasing of rotational and translational degrees of freedom, etc.[43] However, since our aim was to compare the different terbinafine positions in the SE binding pocket each time the same molecules were considered.

To sum up, the most favorable inhibitor−enzyme interactions, along with the fastest achieved convergence during the MD simulations, were observed in the case of the T1_B3 system.

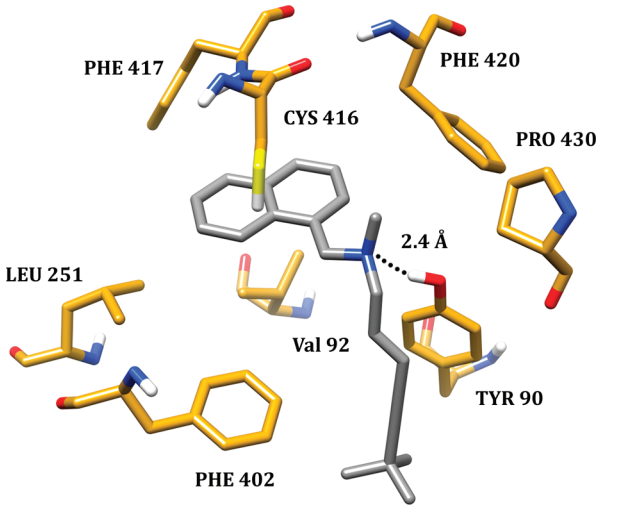

Figure 3. Amino acids crucial for binding terbinafine to *S. cerevisiae* SE. Leu251Phe, Phe402Leu, Phe420Leu, and Phe430Ser point mutations were found to cause terbinafine restance.[30] For Tyr 90, Val 92, Cys 416, and Phe 417, firm interactions with terbinafine were determined (Table 2).

However as it is not possible to simulate accurately all factors present in vivo, there is always a strong need to compare in silico findings with the experimental data. From available experimental reports especially useful for our purpose was the study on the *S. cerevisiae* SE point mutations causing terbinafine resistance.[30] The authors studied 10 mutants of *S. cerevisiae* resistant to terbinafine isolated after chemical or UV mutagenesis. Molecular analysis of these mutants revealed single base pair exchanges in the ERG1 gene coding for the SE. The amino acid changes caused by the point mutations were clustered in two regions of the SE protein. Seven mutants carried the amino acid substitutions in the C-terminal part of the protein, that is Phe402Leu (one mutant), Phe420Leu (one mutant), and Pro430Ser (five mutants). Three mutants carried an Leu251Phe exchange in the central part of the protein. Two mutations that were generated by PCR mutagenesis of the ERG1 gene and that conferred terbinafine resistance were mapped in the same regions of the ERG1 protein, with one resulting in an Leu251Phe exchange and the other resulting in an Phe433Ser exchange. The mutations clearly indicate which regions are responsible for the interaction of SE with terbinafine. Pointed amino acids determine a specific cavity, and terbinafine in the T1_B3 pose, due to its characteristic bend, fits this cavity very well (Figures 2 and 3). No other calculated terbinafine pose corresponded favorably with the experimental findings on terbinafine-resistant mutants.

From among the discussed amino acids, terbinafine interacts the strongest with those located in the C-terminal part of the protein: the Phe 402 and Phe 420 (−7.2 and −8.5 kJ/mol, respectively), by forming with them typical CH/π bonding interactions (Tabel 2, Figure 3). From among the rest of the 48 inspected amino acid−terbinafine pairs, firm attractive interactions were found for Phe 417 (−7.7 kJ/mol) and Cys 416 (−15.9 kJ/mol), also located in the C-terminal part of the protein. The Phe 417 and Cys 416 make CH/π type contacts with the terbinafine aromatic ring. Additionally in the central part of the enzyme binding pocket, Val 92 makes with the terbinafine molecule a set of CH/π attractive interactions (−7.9 kJ/mol). The strongest attraction, however, was determined in the central

Table 2. Calculated Interaction Energies[a] and Distances between Terbinafine and the Amino Acids Included in Quantum Mechanical Calculations

amino acid	E (kJ/mol)	distance (Å)
Glu 60	−1.4	>5
Leu 61	−1.5	3.2
Tyr 90	−32.2	2.4
Thr 91	−0.9	4.4
Val 92	−7.9	3.3
Phe 94	−1.5	3.5
Val 99	−2.0	2.5
Ile 101	0.3	2.2
Tyr 103	−0.7	5
Val 146	−0.1	>5
Hse 246	−0.6	4.8
Gly 247	−1.2	3.1
Hse 248	−1.3	>5
Val 249	−1.5	2.5
Ile 250	−0.7	>5
Leu 251	−1.5	2.3
Pro 257	−0.1	>5
Ile 258	−0.1	>5
Leu 259	−1.0	2.4
Val 260	−0.5	>5
Tyr 261	−0.1	>5
Leu 271	−0.1	>5
Cys 272	0.0	>5
Ala 273	0.0	>5
Arg 313	0.3	>5
Pro 342	−0.5	>5
Leu 343	−2.5	3.1
Thr 344	−0.6	2.8
Gly 345	0.9	2.2
Gly 346	−0.5	3.9
Leu 394	−0.8	4.6
Leu 398	−1.1	2.7
Tyr 399	−0.3	>5
Leu 401	−4.0	2.2
Phe 402	−7.2	2.3
Gln 413	−1.1	2.8
Lys 414	−3.9	4.8
Cys 416	−15.9	2.6
Phe 417	−7.7	2.6
Tyr 419	−1.0	>5
Phe 420	−8.5	2.7
Cys 426	−0.5	>5
Val 427	−0.3	>5
Lys 429	−0.2	>5
Pro 430	−3.0	2.8
Val 431	−0.1	>5
Phe 433	−0.2	>5
Leu 434	−0.1	2.3

[a] Energies were calculated at MP2/6-31G(d) level of theory with the usual counterpoise correction.

part of the enzyme binding pocket (−32.2 kJ/mol) as the Tyr 90 OH group forms a hydrogen bond with the terbinafine amine N atom, and there are $\pi-\pi$ interactions present between the Tyr 90 aromatic ring and the terbinafine ene-yne moiety (Figure 3). As expected the mutation of Tyr 90 to Phe decreased the energy of interaction to −6.8 kJ/mol.

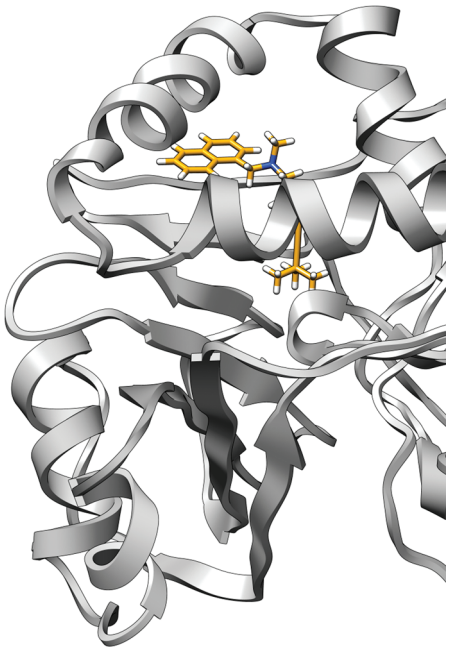

Figure 4. Preferable terbinafine orientation inside the *S. cerevisiae* SE binding pocket. The *tert*-butyl group is oriented toward the protein center.

As we mentioned before, next to the calculated interaction energies there are several other factors that contribute to the overall binging affinity. One of them, presumably the most significant one, is the hydrophobic effect[39] especially in systems consisting of a highly lipophilic ligand and a tight lipophilic pocket, such as the investigated one. For the T1_B3 position, calculated hydrophobic contact surface area between the ligand and the protein equaled to 324 Å^2. Although different authors opt for different values, it is generally accepted that the removal of the hydrophobic surface area from water, by binding to a hydrophobic region of a receptor, is worth a minimum of −0.1 kJ/(Å^2·mol).[44−46] Assuming this value, for the T1_B3 system we obtain an additional contribution to the binging energy, derived by the hydrophobic effect, up to −32.4 kJ.

Inspecting the *S. cerevisiae* squalene epoxidase model, and in particular the substrate binding pocket structure, one can distinguish three regions. In the exterior part of the protein lies a small, highly hydrophobic pocket connected with the main cavity. The main cavity, partly consisting of polar amino acids, leads then toward the FAD binding domain. The third element forms a narrow funnel, which may be an alternative entrance to the active place for natural substrate (squalene). In the T1_B3 position the terbinafine lipophilic moiety is located vertically inside the SE binding pocket with the *tert*-butyl group oriented toward its center. The part of the molecule containing the naftalene ring is hinged and assumes the position inside the small, highly hydrophobic cavity in the upper part of the pocket (Figure 4). Such a position results in the SE conformational changes and prevents the natural substrate from being able to bind to the enzyme active site. The simulation results indicate that for the protein without terbinafine there are two possible ways through which the natural

substrate (squalene) molecule can get into the active site. When terbinafine binds to SE it blocks the first way and changes the geometry of the other. That would explain the experimentally determined shapes of the Lineweaver−Burk plots.[8]

CONCLUSION

Our aim was to propose a mechanism of squalene epoxidase inhibition by terbinafine, and the basic questions were about the inhibitor orientation inside the binding pocket and the role of the terbinafine main structural elements: ene-yne moiety, amine group, and naftalene ring. Consequently, a three-step computational procedure[47] was carried out, resulting in the determination of the preferable way of terbinafine to SE binding. First, based on the SE model, the docking procedure was carried out for the 8 different parameters sets, and in all, 320 terbinafine poses were obtained. From the results, depending mainly on the AutoDock score and rmsd between obtained positions, five positions were chosen for further MM/QM calculation. For the selected terbinafine positions MD simulations were performed next without any constrains from either inhibitor or protein atoms. To avoid computational artifacts during the molecular dynamic simulation, such parameters as rmsd, between the initial and final protein structure as well as the number of steps required to meet convergence criteria were thoroughly inspected. For the T1_B3 system these parameters were the most promising.

Finally the time-averaged structures of inhibitor−enzyme complexes were divided into smaller parts for the quantum mechanical calculations. QM region size was defined by the distance from the terbinafine molecule, and these amino acids were included, where at least one atom was in the range of 5 Å from any of the terbinafine atoms. In all, interaction energies of the 48 terbinafine−amino acid pairs for each different terbinafine orientation in the SE binding pocket were calculated.

The QM region radii (R) of 5 Å seems to be a good choice in such cases as neither increasing (R > 5 Å) nor decreasing (R = 3 Å) the QM region size affected the conclusions.

The data obtained indicated that SE interacts the strongest with the terbinafine molecule in the T1_B3 position (−117 kJ/mol), and these findings seem to correspond to the experimental data pointing to the amino acids crucial for terbinafine binding. The amino acids mark the specific cavity, and terbinafine in the T1_B3 pose, due to its characteristic bend, fits this cavity much better than in any other determined position. From among the five amino acids, where mutation results in terbinafine resistance, during the computational procedure, two were determined as crucial and two as important for binding terbinafine in the T1_B3 positions. Moreover, we observed for the T1_B3 system the lowest rmsd between the initial and final structure and the fastest convergence through the MD simulation, which may further suggest that T1_B3 binding mode of terbinafine is indeed the one leading to inhibition of the SE enzyme.

We found that the strongest interaction between terbinafine and SE stems from hydrogen bonding between hydrogen-bond donors—hydroxyl group of Tyr90 and amine nitrogen atom of terbinafine. Also firm attractive interactions, coming mainly from CH/π type contacts, were identified between terbinafine and Phe 402, Phe 420, Tyr 90, Val 92, Cys 416, and Phe 41.

The T1_B3 pose is a very characteristic one because part of the molecule containing the naftalene ring is in this case hinged and assumes the position inside the small, highly hydrophobic cavity in the upper part of the pocket. The *tert*-butyl moiety of terbinafine points then toward the center of the enzyme, and the whole molecule seems to block the main entrance to the enzymès catalytic site. The simulations indicate that for the protein without terbinafine there are two possible ways through which the natural substrate (squalene) molecule can get into the active site. When terbinafine binds to SE it blocks the first way and changes the geometry of the other, which would clarify the experimentally determined noncompetitive manner of SE inhibition by terbinafine.

Due to the high yeast SE enzymes sequence similarity obtained information may be used for a quick determination of analogue mechanisms in the case of dermatophytes fungi, such as *Trichophyton rubrum* or *C. albicans* and many others. There is also ca. 30% alignment similarity between yeast and mammalian SE enzymes. The latter being the target for designing drugs that may decrease blood cholesterol levels. Thus our results, elucidating at a molecular level the mode of terbinafine inhibitory activity, are likely to be used in designing more potent or selective antifungal drugs or even medicines lowering cholesterol in humans.

ASSOCIATED CONTENT

Supporting Information. *S. cerevisiae* SE model, chosen docked positions of terbinafine, MD simulation results (structures), and QM calculation results (all values of calculated terbinafine−amino acids interaction energies). This information is available free of charge via the Internet at http://pubs.acs.org/.

AUTHOR INFORMATION

Corresponding Author

*M.N.: e-mail marcinn@bioinfo.pl. M.H.: e-mail hoffmann@man.poznan.pl.

ACKNOWLEDGMENT

M.H. and K.G. thank the Foundation for Polish Science for support via FOCUS program. L.R., P.S. and L.S.W. acknowledge support by European Commision grant within 7 Framework Project (OxyGreen; KBBE-2007-212281). The work of D.M.P. and M.L. was supported by the Polish Ministry of Education and Science (grant no. N301 159735). Calculations were performed at the Poznań Supercomputing and Networking Center.

REFERENCES

(1) Jahnke, L.; Klein, H. Oxygen requirements for formation and activity of the squalene epoxidase in Saccharomyces cerevisiae. *J. Bacteriol.* **1983**, *155*, 488–492.

(2) Yamamoto, S.; Bloch, K. Studies on squalene epoxidase of rat liver. *J. Biol. Chem.* **1970**, *245*, 1670–1674.

(3) Tai, H.-H.; Bloch, K. Squalene epoxidase of rat liver. *J. Biol. Chem.* **1972**, *247*, 3767–3773.

(4) Ono, T.; Bloch, K. Solubilization and partial characterization of rat liver squalene epoxidase. *J. Biol. Chem.* **1975**, *250*, 1571–1579.

(5) Ryder, N. S.; Dupont, M.-C. Properties of a particulate squalene epoxidase from Candida albicans. *Biochim. Biophys. Acta* **1984**, *794*, 466–471.

(6) Georgopoulos, A.; Petranyi, G.; Mieth, H.; Drews, J. In vitro activity of naftifine, a new antifungal agent. *Antimicrob. Agents Chemother.* **1981**, *19*, 386–389.

(7) Petranyi, G.; Ryder, N. S.; Stuetz, A. Allylamine Derivatives: New Class of Synthetic Antifungal Agents Inhibiting Fungal Squalene Epoxidase. *Science* **1984**, *224*, 1239–1241.

(8) Ryder, N. S.; Dupont, M.-C. Inhibition of squalene epoxidase by allylamine antimycotic compounds. A comparative study of the fungal and mammalian enzymes. *Biochem. J.* **1985**, *230*, 765–770.

(9) Ruckenstuhl, C.; Poschenel, A.; Possert, R.; Baral, P. K.; Gruber, K.; Turnowsky, F. Structure-Function Correlations of Two Highly Conserved Motifs in Saccharomyces cerevisiae Squalene Epoxidase. *Antimicrob. Agents Chemother.* **2008**, *52*, 1496–1499.

(10) Schreuder, H. A.; Prick, P. A.; Wierenga, R. K.; Vriend, G.; Wilson, K. S.; Hol, W. G.; Drenth, J. Crystal structure of the p-hydroxybenzoate hydroxylase-substrate complex refined at 1.9 A resolution. Analysis of the enzyme-substrate and enzyme-product complexes. *J. Mol. Biol.* **1989**, *208*, 679–696.

(11) Eppink, M. H.; Schreuder, H. A.; Van Berkel, W. J. Identification of a novel conserved sequence motif in flavoprotein hydroxylases with a putative dual function in FAD/NAD(P)H binding. *Protein Sci.* **1997**, *6*, 2454–2458.

(12) Nagai, M.; Sakakibara, J.; Wakui, K.; Fukushima, Y.; Igarashi, S.; Tsuji, S.; Arakawa, M.; Ono, T. Localization of the squalene epoxidase gene (SQLE) to human chromosome region 8q24.1. *Genomics* **1997**, *44*, 141–143.

(13) Hidaka, Y.; Satoh, T.; Kamei, T. J Regulation of squalene epoxidase in Hep G2 cells. *Lipid Res.* **1990**, *31*, 2087–2094.

(14) Sakakibara, J.; Watanabe, R.; Kanai, Y.; Ono, T. Molecular cloning and expression of rat squalene epoxidase. *J. Biol. Chem.* **1995**, *270*, 17–20.

(15) Kosuga, K.; Hata, S.; Osumi, T.; Sakakibara, J.; Ono, T. Nucleotide sequence of a cDNA for mouse squalene epoxidase. *Biochim. Biophys. Acta* **1995**, *1260*, 345–348.

(16) Laden, B. P.; Tang, Y.; Porter, T. D. Cloning, heterologous expression and enzymological characterization of human squalene monooxygenase. *Arch. Biochem. Biophys.* **2000**, *374*, 381–388.

(17) Horie, M.; Tsuchiya, Y.; Hayashi, M.; Iida, Y.; Iwasawa, Y.; Nagata, Y. NB-598: a potent competitive inhibitor of squalene epoxidase. *J. Biol. Chem.* **1990**, *5*, 18075–18078.

(18) Horie, M.; Sawasaki, Y.; Fukuzumi, H.; Watanabe, K.; Iizuka, Y.; Tsuchiya, Y.; Kamei, T. Hypolipidemic effects of NB-598 in dogs. *Atherosclerosis* **1991**, *88*, 183–192.

(19) Gotteland, J. P.; Brunel, I.; Gendre, F.; Desire, J.; Delhon, A.; Junquero, D.; Oms, P.; Halazy, S. (Aryloxy)methylsilane derivatives as new cholesterol biosynthesis inhibitors: synthesis and hypocholesterolemic activity of a new class of squalene epoxidase inhibitors. *J. Med. Chem.* **1995**, *38*, 3207–3216.

(20) Gotteland, J. P.; Loubat, C.; Planty, B.; Junquero, D.; Delhon, A.; Halazy, S.; Bioorg. Sulfonamide derivatives of benzylamine block cholesterol biosynthesis in HepG2 cells: a new type of potent squalene epoxidase inhibitors. *Med. Chem. Lett.* **1998**, *8*, 1337–1342.

(21) Chugh, A.; Ray, A.; Gupta, J. B. Squalene epoxidase as hypocholesterolemic drug target revisited. *Prog. Lipid Res.* **2003**, *42*, 37–50.

(22) Sawada, M.; Matsuo, M.; Hagihara, H.; Tenda, N.; Nagayoshi, A.; Okumura, H.; Washizuka, K.; Seki, J.; Goto, T. Effect of FR194738, a potent inhibitor of squalene epoxidase, on cholesterol metabolism in HepG2 cells. *Eur. J. Pharmacol.* **2001**, *431*, 11–16.

(23) Koskiniemi, H.; Metsä-Ketelä, M.; Dobritzsch, D.; Kallio, P.; Korhonen, H.; Mäntsälä, P.; Schneider, G.; Niemi, J. Crystal structures of two aromatic hydroxylases involved in the early tailoring steps of angucycline biosynthesis. *J. Mol. Biol.* **2007**, *372*, 633–648.

(24) Schreuder, H. A.; Prick, P.; Wierenga, R. K.; Vriend, G.; Wilson, K.; Hol, W. G. J.; Drenth, J rystal structure of the p-hydroxybenzoate hydroxylase-substrate complex refined at 1.9 A resolution. Analysis of the enzyme-substrate and enzyme-product complexes. *J. Mol. Biol.* **1989**, *208*, 679–696.

(25) Ginalski, K.; Elofsson, A.; Fischer, D.; Rychlewski, L. 3D-Jury: a simple approach to improve protein structure predictions. *Bioinformatics* **2003**, *19*, 1015–1018.

(26) Fox, T.; Kollman, P. A. The application of different solvation and electrostatic models in molecular dynamics simulations of ubiquitin: how well is the X-ray structure "maintained"?. *Proteins* **1996**, *25*, 315–334.

(27) MacKerell, A. D., Jr.; et al. All-atom empirical potential for molecular modeling and dynamics studies of proteins. *J. Phys. Chem. B* **1998**, *102*, 3586–3616.

(28) Morris, G. M.; Goodsell, D. S.; Halliday, R. S.; Huey, R.; Hart, W. E.; Belew, R. K.; Olsen, A. J. Automated Docking Using a Lamarckian Genetic Algorithm and and Empirical Binding Free Energy Function. *J. Comput. Chem.* **1998**, *19*, 1639–1662.

(29) Marvin and Calculator Plugins 2008, ChemAxon

(30) Leber, R.; Fuchsbichler, S.; Klobuníková, V.; Schweighofer, N.; Pitters, E.; Wohlfarter, K.; Lederer, M.; Landl, K.; Ruckenstuhl, Ch.; Hapala, I.; Turnowsky, F. Molecular mechanism of resistance to terbinafine in Saccharomyces cerevisiae. *Antimicrob. Agents Chemother.* **2003**, *47*, 3890–3900.

(31) Kale, L.; Skeel, R.; Bhandarkar, M.; Brunner, R.; Gursoy, A.; Krawetz, N.; Phillips, J.; Shinozaki, A.; Varadarajan, K.; Schulten, K. NAMD2: Greater Scalability for Parallel Molecular Dynamics. *J. Comput. Phys.* **1999**, *151*, 283–312.

(32) Humphrey, W.; Dalke, A.; Schulten, K VMD: visual molecular dynamics. *J. Mol. Graphics* **1996**, *14*, 33–38.

(33) Vanommeslaeghe, K.; Hatcher, E.; Acharya, C.; Kundu, S.; Zhong, S.; Shim, J.; Darian, E.; Guvench, O.; Lopes, P.; Vorobyov, I.; MacKerell, A. D. CHARMM general force field: A force field for drug-like molecules compatible with the CHARMM all-atom additive biological force fields. *J. Comput. Chem.* **2010**, *31*, 671–690.

(34) Grubmüller, H.; Heymann, B.; Tavan, P. Ligand Binding: Molecular Mechanics Calculation of the Streptavidin-Biotin Rupture Force. *Science* **1996**, *271*, 997–999.

(35) Frisch, M. J.; Trucks, G. W.; Schlegel, H. B.; Scuseria, G. E.; Robb, M. A.; Cheeseman, J. R.; Montgomery, Jr., J. A.; Vreven, T.; Kudin, K. N.; Burant, J. C.; Millam, J. M.; Iyengar, S. S.; Tomasi, J.; Barone, V.; Mennucci, B.; Cossi, M.; Scalmani, G.; Rega, N.; Petersson, G. A.; Nakatsuji, H.; Hada, M.; Ehara, M.; Toyota, K.; Fukuda, R.; Hasegawa, J.; Ishida, M.; Nakajima, T.; Honda, Y.; Kitao, O.; Nakai, H.; Klene, M.; Li, X.; Knox, J. E.; Hratchian, H. P.; Cross, J. B.; Bakken, V.; Adamo, C.; Jaramillo, J.; Gomperts, R.; Stratmann, R. E.; Yazyev, O.; Austin, A. J.; Cammi, R.; Pomelli, C.; Ochterski, J. W.; Ayala, P. Y.; Morokuma, K.; Voth, G. A.; Salvador, P.; Dannenberg, J. J.; Zakrzewski, V. G.; Dapprich, S.; Daniels, A. D.; Strain, M. C.; Farkas, O.; Malick, D. K.; Rabuck, A. D.; Raghavachari, K.; Foresman, J. B.; Ortiz, J. V.; Cui, Q.; Baboul, A. G.; Clifford, S.; Cioslowski, J.; Stefanov, B. B.; Liu, G.; Liashenko, A.; Piskorz, P.; Komaromi, I.; Martin, R. L.; Fox, D. J.; Keith, T.; Al-Laham, M. A.; Peng, C. Y.; Nanayakkara, A.; Challacombe, M.; Gill, P. M. W.; Johnson, B.; Chen, W.; Wong, M. W.; Gonzalez, C.; and Pople, J. A. *Gaussian 03*, revision C.02; Gaussian, Inc.: Wallingford, CT, 2004.

(36) Møller, C.; Plesset, M. S. Note on an Approximation Treatment for Many-Electron Systems. *Phys. Rev.* **1934**, *46*, 618–622.

(37) Jensen, F. Polarization consistent basis sets. III. The importance of diffuse functions. *J. Chem. Phys.* **2002**, *117*, 9234–9240.

(38) Boys, S. F.; Bernardi, F. The calculation of small molecular interactions by the differences of separate total energies. Some procedures with reduced errors. *Mol. Phys.* **1970**, *19*, 553–566.

(39) Southall, N. T.; Dill, K. A.; Haymet, A. D. J. A View of the Hydrophobic Effect. *J. Phys. Chem. B* **2002**, *106*, 521–533.

(40) Collaborative Computational Project. The CCP4 Suite, No. 4. Programs for Protein Crystallography. *Acta Crystallogr.* **1994**, *D50*, 760–763.

(41) Pettersen, E. F.; Goddard, T. D.; Huang, C. C.; Couch, G. S.; Greenblatt, D. M.; Meng, E. C.; Ferrin, T. E. UCSF Chimera--a visualization system for exploratory research and analysis. *J. Comput. Chem.* **2004**, *25*, 1605–1612.

(42) Khandelwal, A.; Lukacova, V.; Comez, D.; Kroll, D. M.; Raha, S. Balaz A combination of docking, QM/MM, and MD simulation for binding affinity estimation of metalloprotein ligands. *J. Med. Chem.* **2005**, *48*, 5437–5447.

(43) Brandsdal, B. O.; Österberg, F.; Almlöf, M.; Feierberg, I.; Luzhkov, V. B.; Åqvist, J. Free Energy Calculations and Ligand Binding. *Adv. Protein Chem.* **2003**, *66*, 123–158.

(44) Davis, A. M.; Teague, S. J. Hydrogen Bonding, Hydrophobic Interactions, and Failure of the Rigid Receptor Hypothesis. *Angew. Chem., Int. Ed.* **1999**, *38*, 736–749.

(45) Böhm, H. J. The development of a simple empirical scoring function to estimate the binding constant for a protein-ligand complex of known three-dimensional structure. *J. Comput.-Aided Mol. Des.* **1994**, *8*, 243–256.

(46) Williams, D. H.; Cox, J. P. L.; Doig, A. J.; Gardner, M.; Cerhard, U.; Kaye, P. T.; Lal, A. R.; Nicholls, I. A.; Salter, C. J.; Mitchellf, R. C. Toward the Semiquantitative Estimation of Binding Constants. Guides for Peptide-Peptide Binding in Aqueous Solution. *J. Am. Chem. Soc.* **1991**, *113*, 7020–7030.

(47) Hoffmann, M.; Eitner, K.; von Grotthuss, M.; Rychlewski, L.; Banachowicz, E.; Grabarkiewicz, T.; Szkoda, T.; Kolinski, A. Three dimensional model of severe acute respiratory syndrome coronavirus helicase ATPase catalytic domain and molecular design of severe acute respiratory syndrome coronavirus helicase inhibitors. *J. Comput.-Aided Mol. Des.* **2006**, *20*, 305–319.